© 2018 IJSRSET | Volume 4 | Issue 1 | Print ISSN: 2395-1990 | Online ISSN : 2394-4099
Themed Section : Engineering and Technology

A Novel Local Line Binary Pattern Based Image Segmentation Algorithm for Defocus Blur

Y. Meenakshi[1], B. Anuradha[2]
[1]M.Tech, S.V.U.College of Engineering, S.V.U, Tirupati, Andhra Pradesh, India
[2]Professor, ECE Department S.V.U, Tirupati, Andhra Pradesh, India

ABSTRACT

When an image is captured with the aid of any optical imaging gadgets in that picture, defocus blur is the not unusual unwanted aspect. It is either beautify or inhibit the ocular percept of an photograph scene. In unique photograph processing operations like photograph recovery and object detection we needed to seperate the partly blurred photograph into blurred and non-blurred areas. We suggested a sharpness metric in this document based totally on LBP and a robust segmentation algorithmic program for the defocus blur. The proposed sharpness metric exploits the observation that the majority neighborhood image patches in blurred regions have considerably lesser of bounds native binary patterns as compared with the ones in sharp regions. Mistreatment this metric, beside photograph matting and multiscale inference, we have a tendency to acquire tremendous sharpness maps. Tests on several partly blurred images have been accustomed to examine our blur segmentation algorithmic process and 6 comparative methods. The consequences display that our proposed method for defocus blur achieves comparative segmentation outcomes with the state of the artwork and have the big pace gain over the others. LLBP results will be improved for proposed work.

Keywords: DIP ,LBP,Sharpness,Photograph recovery,Object detection ,LLBP.

I. INTRODUCTION

Defocus estimation plays a critical function in computer imaginative and prescient and computer portraits programs together with depth estimation, picture awesome evaluation, picture deblurring and refocusing. Different conventional techniques have implemented on more than one snap shots for defocussing. A some of pictures are the same view is captured with the usage of a couple of recognition settings. Then the defocus is measured in some unspecified time in the subsequent of a implicit or unique deblurring gadget. Recently, picture pairs captured using encoded aperture cameras [5] are used for higher defocus blur diploma and all-centered photo restoration. However, these techniques be troubled by way of the occlusion trouble and require the scene to be static, which limits their programs in exercise.

Estimating defocus blur is a tough mission mainly beacause of the fact the corresponding PSFs are spatially numerous and can not be represented via any worldwide descriptor. Indeed, spatially varying defocus PSFs for a taken digicam may be pre-calculated and defined typically thru a simple version (e.g. Disc, Gaussian) and it is characterized with one parameter which shows the scale of PSFs (radius, large deviation). For an picture, we calls the 2D map of the scale parameter the defocus blur map, which suggests the extent of nearby blur at each pixel (see Figure 1). The foremost reason of this paper is to offer an automatic manner of estimate a defocus blur map from a single input photograph.

Nonfocus blur estimation map has several functionality applications. For instance, it could be employed to discover and phase in-recognition topics from the external historical past, helping a photograph editor to edit the problem of hobbies or the history, one after the other. Besides that, nonfocus blur degree is in element refers the depth of the scene, a blur map also affords vital records for intensity estimation. The computation of depth information commonly calls for pics of the identical scene taken in the particular time, however from slightly precise vantage points, i.e., A stereographic pair [6]. However, in maximum times most effective one photo is available. A blur map lets in one to reconstruct a three-D scene from a photo as long as the virtual camera settings (focal period, aperture settings, and so on) are known. For picture restoration applications, if each the defocus PSF calibration and blur estimation maps are made, we are capable to reconstruct an all in-attention picture thru a nonblind spatially different deblurring procedure.

This method regionally selects the best PSF thru comparing its deconvolution mistakes. It needs a especially designed aperture filter out for the digital camera, which strongly limits its vicinity of utility. Instead of evaluting the maximum ideal blur scale in the non-forestall area, it could most effective become aware about the most possibly candidate from a finite type of calibrated PSFs with virtually restricted accuracy. Chakrabartiet al. Counseled a technique estimating the chance feature of a given candidate PSF primarily based on nearby frequency aspect analysis with out deconvolution [8]. In their paper, the approach is implemented to discover simple movement blur, however it is able to also be hired for defocus blur identity. Again it could best discover top-rated PSFs from a finite quantity of candidates.

II. LITERATURE SURVEY

Fergus et al. [1] Proposed a method that camera shakes in the focussing of exposure may causes to objectionable photograph blur and harm pix. Conventional blind deconvolution strategies not often count on frequency-area parameters on pics for the motion course at the similar time as camera shake. Real digital camera motions can observe up the convoluted way and spatial place preceding can better keeps visually photograph residences. They introduced a method to dispose of the results of digital digicam shake from blurred pics. This approach assumes that a uniform digital digicam blur over the picture and additionally negligible in-plane digicam rotation. In this method to be calculate the blur from the digital digicam shake, the individual want to specify an image place without saturation effects.They confirmed consequences for a wide type of virtual photographs which can captured from private photograph collections.

Bae and Durand[2] provided the picture processing techniques in which defocus magnification is used to perform blur estimation. To optimize defocus blur suitable to lens aperture with the aid of taking a single photo then estimate the size of blur kernel at edges and similarly they unfold this method to the whole image. In this method multi scale component detector is used and version turning into that attain the size of blur propagate the blur degree thru assuming that fogginess is simple in which depth and coloration are approximately comparable. Using defocus map, they extend the present blurness, which means that blur the blurred region and keeps the pointy areas sharp. In assessment to other techniques extra difficult problems arises which includes depth from defocus, so this proposed method do no longer need precise depth estimation and do no longer need to disambiguate texture plenty less areas. The technique models changes in power the least bit frequencies with blur and no longer just extremely high frequenies (edges).

Levin et al. [3] Observe blind deconvolution method that's the recovery of a pointy version from a blurred photo while the blur kernel isn't always regarded. Most algorithms have dramatic progress; despite the facts that many additives of the problem remain hard

and difficult to understand. The object of this approach is to investigate and compare blind deconvolution algorithms each theoretically further to experimentally. They had additionally noted the failures of the MAP approaches.

Kee et al. [4], Mentioned that considerable blur is generated because of the optical device of the digicam, moreover with professional lenses. They introduce technique to diploma the blurred kernel thickly over the image and additionally for the duration of multi aperture and zoom settings. It proven that the blur kernel may have a non-negligible unfold, even with among the finest equipment. The spatial changes are not regularly symmetrical and not even left-right symmetric .In this method fashions of the optic blur are evolved and compared each having advantages respectively. It is established that the version discover correct blur kernel that may be used to repair images. They set up that they're capable of produce snap shots which can be more uniformly sharp then the ones pictures which produced with spatially-invariant deblurring technique.

Tai and brown in [5] As Image defocus estimate is usable for numerous applications along with deblurring, blur growth, measuring picture fine, and intensity of situation segmentation. They proposed a easy effective technique for estimates a defocus blur map primarily based on the relationship of the evaluation to the image gradient in a neighborhood photograph region and speak to this relationship the community contrast earlier. The gain of this technique is that it does no longer need filter out banks or frequency decomposition[5] of the enter picture; infact it handiest wishes to examine nearby gradient profiles with the neighborhood assessment. They speak the concept behind the nearby evaluation preceding and tested its outcomes on a various of experiments. And it's determined that for herbal in-recognition images, this distribution follows a comparable pattern. They examined this distribution via plotting the circulation of the LC in photographs suffered from special form of deterioration. This earlier is useful in estimating defocus blur, in segmenting in attention areas from depth-of-area image and in score photo pleasant.

III. PROPOSED METHOD

Linear Binary Patterns(LBP):

LBP patterns were a hit for laptop vision problems which includes texture segmentation, face reputation, historic past subtraction and popularity of 3d texture surfaces [36]. The LBP code of pixel (x_c,y_c) is define as

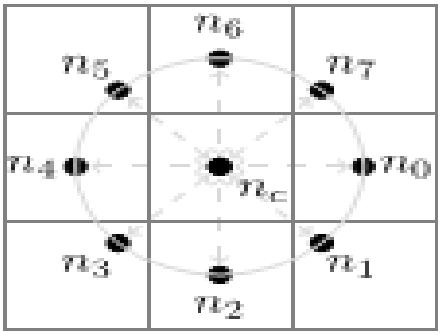

Figure 1. 8-bit LBP with P=8,R=1.

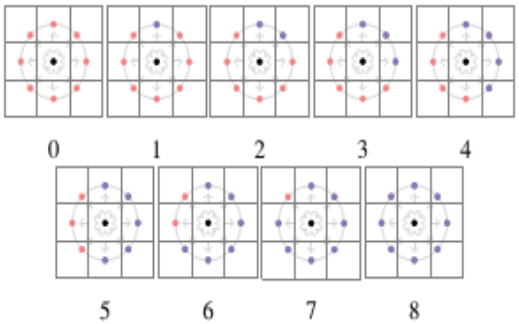

Figure 2. Uniform rotationally invariant LBP.

$$LBP_{P,R}(x_c, y_c) = \sum_{p=0}^{P-1} S(n_p - n_c) \times 2^P$$

With $S(x) = \begin{cases} 1 & |x| \geq T_{LBP} \\ 0 & |x| < T_{LBP} \end{cases}$ (3.1)

Where c is depth of the first pixel (x_c,y_c), n_p corresponding intensity of the P neighboring pixels placed on a circle of radius R focused at n_c, and T_{LBP}>zero is a small, high excellent threshold that permit to you accumulate robustness for flat image regions as in [9]. Figure.2 indicates the places of the neighboring pixels n_p for P=eight and R=1. In widespread, the point's n_p don't fall within the middle

of image pixels, so the intensity of n_p is acquired with bilinear interpolation[7]. A rotation invariant version of LBP can be finished via acting the round bitwise proper shift that minimizes the fee of the LBP code at the similar time as it's miles taken as a binary range.

In this manner, number of specific styles are reduced to 36. Ojala et al. Observed that now not all rotation invariant styles sustain rotation equally well [4], and so proposed the use of simplest uniform styles which may be a subset of the rotation invariant patterns. A sample is uniform if the round collection of bits consists of no more than transitions from one to 0, or 0 to one. The nonuniform patterns are then all dealt with as one single sample. This further reduces the variety of particular patterns to 10 (for 8-bit LBP), that is, 9 uniform patterns, and the class of nonuniform patterns[6]. The uniform styles are verified in Figure two. In this decide, neighboring pixels are colored blue if their intensity distinction from centre pixel is bigger than T_{LBP}, and we are saying that it is been "delivered approximately", otherwise, the neighbours are coloured crimson.

Our proposed sharpness metric exploits those observations:

$$m_{LBP} = \frac{1}{N}\sum_{i=6}^{9} n\left(LBP_{8,1}^{riu2}i\right) \qquad (3.2)$$

Where $n\left(LBP_{8,1}^{riu2}i\right)$ is the amount of rotation invariant of the uniform eight-bit LBP sample of kind i, and N is the overall amount of pixels within the determined on community vicinity which serves to normalize the metric so that $m_{LBP} \in [0,1]$. One of the advantage of measuring sharpness in the LBP area is that LBP capabilities are strong to monotonic illumination modifications which stand up regularly in herbal photos. The threshold LBP in Equation (3.1) control the projected metric's sensitivity to sharp region.

Local Line Binary Pattern(LLBP):

The LLBP is prompted from Local Binary Pattern (LBP), the advantage of LLBP operator is that the modifications in image intensity like vertices,edges and corners can be highlighted. The LLBP contains of 2 elements: horizontal and vertical elements. The binary values for the vertical and horizontal components are calculated, by using these binary codes the magnitude of LLBP is calculated. The illustration of LLBP operator is shown in Figure 3, and its mathematic definitions[12] are given in Equations (3.4)-(3.5). $LLBP_h$, $LLBP_v$ & $LLBP_m$ are LLBP on horizontal & vertical direction, and their magnitudes, correspondingly. N refers the line length in picture element, h_n refers the pixel along with the horizontal line and v_n refers the pixel along with the vertical line, c =N_2 is the middle pixel position, h_c on the horizontal line and v_c on the vertical line, and s(·) function defines a limiting function as in Equation (3.3). By using Eq's (3.3) & (3.4), the horizontal element of LLBP ($LLBP_h$) takes a binarycode of N – 1 bits for each picture element.The similar values of bits are taken by the vertical component of LLBP ($LLBP_v$) using Eq's (3.3) and (3.5).

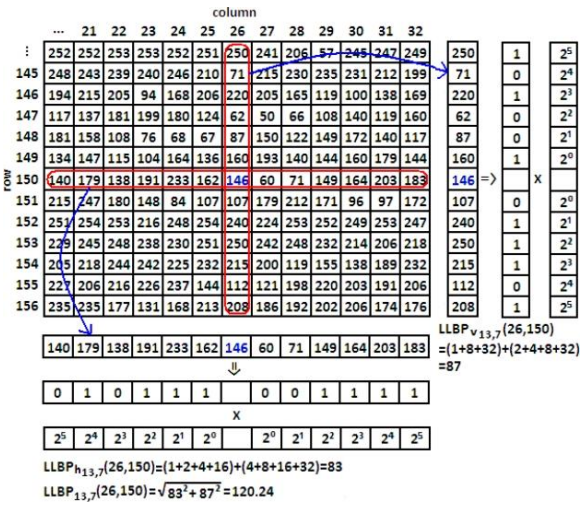

Figure 3. Example of LLBP operator.

$$s(x) = \begin{cases} 1, & x \geq 0 \\ 0, & x < 0 \end{cases} \qquad (3.3)$$

$$LLBP_{h\,N,c}(x,y) = \sum_{n=1}^{c-1} s(h_n - h_c).2^{c-n-1} + \sum_{n=c+1}^{N} s(h_n - h_c).2^{n-c-1} \qquad (3.4)$$

$$LLBP_{h\,N,c}(x,y) = \sum_{n=1}^{c-1} s(v_n - v_c).2^{c-n-1} + \sum_{n=c+1}^{N} s(v_n - v_c).2^{n-c-1} \qquad (3.5)$$

$$LLBP_m = \sqrt{LLBP_{2h} + LLBP_{2v}} \qquad (3.6)$$

Consequently, by combining the binary values from $LLBP_h$ and $LLBP_v$, the total binary value of LLBP for each pixel is 2(N – 1) bits. In Figure 3,the binary

sequence for horizontal (vertical) component is defined from left (top) as 010111001111(2) (101001011101(2)). Hence, the binary value for LLBP is 010111001111101001011101(2).

NEW BLUR SEGMENTATION ALGORITHM

This section gives our set of rules for segmenting blurred/sharp areas with our LBP-based totally sharpness metric, it is summary in Figure.four. The set of regulations has four vital steps: multi-scale sharpness map technology, alpha matting initialization, alpha map computation, and multi-scale inference.

A.Multi-Scale Sharpness Map Generation

In step one, multiple-scale sharpness maps are generated by the usage of m_LBP. The sharpness metric is computed for a close-by patch about each photo pixel. Sharpness maps are built at three scales in which scale refers to close by patch length. By the use of an vital photo [5], sharpness maps can be calculate in constant time in step with pixel for a fixed P and R.

B.Alpha Matting Initialization

Alpha matt is the manner of decomposing an photograph into foreground and ancient beyond. The photograph formation version can be explicitly as

$$I(x,y) = \alpha_{x,y}F(x,y) + \left(1-\alpha_{x,y}\right)B(x,y) \quad (3.7)$$

Where the alfa matte, α x,y, is the opacity cost on pixel role (x,y). It may be interpreted because the self assurance that a picture element is inside the foreground. Typically, alpha matting requires a person to interactively mark acknowledged foreground and history pixels, initializing those pixels with α =1 and α =zero, respectively. Interpreting "foreground" as "sharp" and background as "blurred", we initialized the alpha matting process robotically with the aid of applying a double threshold to the sharpness maps computed inside the preceding step to give up an initial price of α for each picture element.

$$mask^s(x,y) = \begin{cases} 1, & if\, m_{LBP}(x,y) > T_{m_1} \\ 0, & if\, m_{LBP}(x,y) < T_{m_1} \\ m_{LBP}(x,y), & otherwise. \end{cases} \quad (3.8)$$

Where s indexes the dimensions, this is, masks (x,y) is the initial α-map on the s-th scale.

C.Alpha Map Computation

The α-map was solved by minimizing the following cost function as proposed by Levin[8]

$$E(\alpha) = \alpha^T \boldsymbol{L}\alpha + \lambda(\alpha-\hat{\alpha})^T(\alpha-\hat{\alpha}) \quad (3.9)$$

Where α is the vectorized α-map, α^=[mask]^i (X,Y) is one of the vectorized initialize alfa maps from the last step, and L is the matte Laplacian matrix. First time period is the law term that ensures smoothness, and the second one is the facts becoming term that encourages similarity to α^ [10]. For extra details on Equation (3.8), the very last alpha map at every scale is designated as α_s ,s =1,2,three.

D. Multi-Scale Inference

After figure out of the alpha map at three distinct scales, a multiple-scale graphical version became followed to making the final decision[11]. The general electricity at the graphical version is expressed as

$$E(h) = \sum_{s=1}^{3}\sum_i \left|h_i^s - \hat{h}_i^s\right| + \beta\left(\sum_{s=1}^{3}\sum_i\sum_{j\in N_i^s}\left|h_i^s - h_j^s\right| + \sum_{s=1}^{2}\sum_i\left|h_i^s - h_i^{s+1}\right|\right) \quad (3.10)$$

Where $\hat{h}_i^s = \alpha_i^s$ is the alpha map for scale s at pixel area i that become computed inside the preceding step, and $\hat{h}_i^s$ is the sharp region to be inferred. First time period at the proper hand aspect is the unary term that's the price of assigning sharpness cost to $\hat{h}_i^s$ to pixel i in scale s. The second is the pairwise time period which enforces smoothness within the identical scale and throughout different scales. The weight β regulates the comparative importance of those two terms. Optimization of Equation (3.10)

became finished using crazy perception propagation[7].

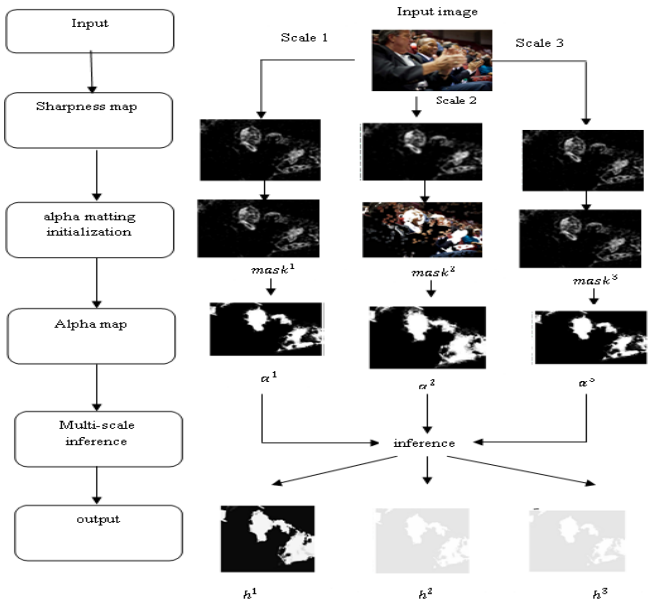

Figure 4. Our blur segmentation algorithm. The output of the algorithm is h 1

The output of the set of rules is h^one which is the inferred sharpness map at the most important scale. This is a grayscale photo, in which better depth shows greater sharpness.

IV. SIMULATION RESULTS

Figure 5 : Segmentation with LBP

Figure 6 : Segmentation with LLBP

Where figure.5. shows the plartially blurred image and it's segmented image, in that segmented image black colour region refers to background and white colour refers to foreground of the input image for local binary pattern image segmentation. Figure.6. shows the plartially blurred image and it's segmented image, in that segmented image black colour region refers to background and white colour refers to foreground of the input image for LLBP image segmentation.

V. CONCLUSION

We efficaciously proposed easy and effective sharpness metric for the segmentation of partly blurred image into blurred and non blurred areas. This metric is frequently based on the distributing of uniform LBP styles in blurred and non blurred areas. The direct use of a few sharpness diploma based at the sparse illustration offers the comparative results to our proposed approach. By integration the metric proper into a multiscale statistics propagation frame work, it can achieve comparative results with state of artwork.

We've confirmed that by using an automatically and adaptively selected threshold Tseg, the algorithm performance is maintained. Our sharpness metric measures the quantity of wonderful LBP patterns in the local neighbourhood so is with performance enforced with the aid of manner of critical images. If combined with real time matting algorithms, inclusive of GPU implementations of worldwide matting [8], our approach would have immoderate pace gain over the other defocus segmentation algorithms.

VI. REFERENCES

[1]. R. Achanta, S. Hemami, F. Estrada, and S. Susstrunk, "Frequency-tuned salient region detection," in Proc. IEEE Conf. Comput. Vis. Pattern Recognit. (CVPR), Jun. 2009, pp. 1597-1604.

[2]. H.-M. Adorf, "Towards HST restoration with a space-variant PSF, cosmic rays and other missing data," in Proc. Restoration HST Images Spectra-II, vol. 1. 1994, pp. 72-78.

[3]. T. Ahonen, A. Hadid, and M. Pietikäinen, "Face description with local binary patterns: Application to face recognition," IEEE Trans. Pattern Anal. Mach. Intell., vol. 28, no. 12, pp. 2037-2041, Dec. 2006.

[4]. S. Bae and F. Durand, "Defocus magnification," Comput. Graph. Forum, vol. 26, no. 3, pp. 571-579, 2007.

[5]. K. Bahrami, A. C. Kot, and J. Fan, "A novel approach for partial blur detection and segmentation," in Proc. IEEE Int. Conf. Multimedia Expo (ICME), Jul. 2013, pp. 1-6.

[6]. J. Bardsley, S. Jefferies, J. Nagy, and R. Plemmons, "A computational method for the restoration of images with an unknown, spatially-varying blur," Opt. Exp., vol. 14, no. 5, pp. 1767-1782, 2006.

[7]. A. Buades, B. Coll, and J.-M. Morel, "A non-local algorithm for image denoising," in Proc. IEEE Comput. Soc. Conf. Comput. Vis. Pattern Recognit. (CVPR), vol. 2. Jun. 2005, pp. 60-65.

[8]. G. J. Burton and I. R. Moorhead, "Color and spatial structure in natural scenes," Appl. Opt., vol. 26, no. 1, pp. 157-170, 1987.

[9]. A. Chakrabarti, T. Zickler, and W. T. Freeman, "Analyzing spatially-varying blur," in Proc. IEEE Conf. Comput. Vis. Pattern Recognit. (CVPR), Jun. 2010, pp. 2512-2519.

[10]. T. S. Cho, "Motion blur removal from photographs," Ph.D. dissertation, Dept. Elect. Eng. Comput. Sci., Massachusetts Inst. Technol., Cambridge, MA, USA, 2010.

[11]. F. Couzinie-Devy, J. Sun, K. Alahari, and J. Ponce, "Learning to estimate and remove non-uniform image blur," in Proc. IEEE Conf. Comput. Vis. Pattern Recognit. (CVPR), Jun. 2013, pp. 1075-1082.

[12]. S. Dai and Y. Wu, "Removing partial blur in a single image," in Proc. IEEE Conf. Comput. Vis. Pattern Recognit. (CVPR), Jun. 2009, pp. 2544-2551.

[13]. R. Fergus, B. Singh, A. Hertzmann, S. T. Roweis, and W. T. Freeman, "Removing camera shake from a single photograph," ACM Trans. Graph., vol. 25, no. 3, pp. 787-794, 2006.

[14]. A. Levin, Y. Weiss, F. Durand, and W. T. Freeman, "Understanding and evaluating blind deconvolution algorithms," in Proc. IEEE Conf. Comput. Vis. Pattern Recognit. (CVPR), Jun. 2009, pp. 1964-1971.